energy&fuels

Article

pubs.acs.org/EF

Combustion of Biosolids in a Bubbling Fluidized Bed, Part 1: Main Ash-Forming Elements and Ash Distribution with a Focus on Phosphorus

Nils Skoglund,*[,†] Alejandro Grimm,[‡] Marcus Öhman,[‡] and Dan Boström[†]

[†]Thermochemical Energy Conversion Laboratory, Department of Applied Physics and Electronics, Umeå University, SE-901 87 Umeå, Sweden

[‡]Energy Engineering, Department of Engineering Sciences & Mathematics, Luleå University of Technology, SE-971 87 Luleå, Sweden

ABSTRACT: This is the first in a series of three papers describing combustion of biosolids in a 5-kW bubbling fluidized bed, the ash chemistry, and possible application of the ash produced as a fertilizing agent. This part of the study aims to clarify whether the distribution of main ash forming elements from biosolids can be changed by modifying the fuel matrix, the crystalline compounds of which can be identified in the raw materials and what role the total composition may play for which compounds are formed during combustion. The biosolids were subjected to low-temperature ashing to investigate which crystalline compounds that were present in the raw materials. Combustion experiments of two different types of biosolids were conducted in a 5-kW benchscale bubbling fluidized bed at two different bed temperatures and with two different additives. The additives were chosen to investigate whether the addition of alkali (K_2CO_3) and alkaline-earth metal ($CaCO_3$) would affect the speciation of phosphorus, so the molar ratios targeted in modified fuels were P:K = 1:1 and P:K:Ca = 1:1:1, respectively. After combustion the ash fractions were collected, the ash distribution was determined and the ash fractions were analyzed with regards to elemental composition (ICP-AES and SEM-EDS) and part of the bed ash was also analyzed qualitatively using XRD. There was no evidence of zeolites in the unmodified fuels, based on low-temperature ashing. During combustion, the biosolid pellets formed large bed ash particles, ash pellets, which contained most of the total ash content (54%−95% (w/w)). This ash fraction contained most of the phosphorus found in the ash and the only phosphate that was identified was a whitlockite, $Ca_9(K,Mg,Fe)(PO_4)_7$, for all fuels and fuel mixtures. With the addition of potassium, cristobalite (SiO_2) could no longer be identified via X-ray diffraction (XRD) in the bed ash particles and leucite ($KAlSi_2O_6$) was formed. Most of the alkaline-earth metals calcium and magnesium were also found in the bed ash. Both the formation of aluminum-containing alkali silicates and inclusion of calcium and magnesium in bed ash could assist in preventing bed agglomeration during co-combustion of biosolids with other renewable fuels in a full-scale bubbling fluidized bed.

1. INTRODUCTION

As the world's population grows larger, it becomes increasingly important to manage and recycle nutrients from biomass back to soil for a more sustainable food and energy production. Recycling ash from renewable fuels is one way to improve element recovery to facilitate a sustainable biomass production. A resource that is related to biomass production in agriculture is municipal sewage sludge, also known as biosolids after further treatment such as digestion. This waste stream resource contains a lot of energy, even after biogas production through digestion, and the high content of macronutrients in biosolids makes it interesting both as a sustainable nutrient resource for new crops and as a co-combustion fuel where the ash produced also could be used as a nutrient resource.[1−5] Incineration of biosolids has the benefits of energy recovery, destruction of both pathogens and anthropogenic chemicals (e.g., pharmaceutical agents and persistent organic pollutants)[6−8] with the possibility of creating an ash with macronutrients available for plants.[5,9,10]

Several studies have shown that biosolids can improve the combustion properties of biomass by reducing the risk of corrosion and fouling, reducing bed agglomeration tendencies and possibly enabling a higher process temperature for some problematic fuels.[11−15] Even if the high ash content in biosolids may pose a challenge for monocombustion it also means that relatively small amounts of biosolids in co-combustion scenarios will have a large impact on the overall ash chemistry.[11,14−16]

How ash can be turned into a resource of macronutrients after combustion and how it affects the thermal energy conversion plant should be considered when designing a co-combustion fuel mixture. As one of the main ash-forming elements in renewable fuels, phosphorus may play an important role in the behavior of fuel ash, depending on its total concentration.[12,13,15,17−22] Biosolids typically contain a lot of phosphorus, compared to renewable fuels in general.[23] One way of recovering phosphorus from these biosolids is to incinerate the biosolid either by monocombustion or co-combustion and use the resulting ash as a nutrient source. If co-combustion is made with other waste streams from food production, it could be possible to improve recycling of phosphorus and other nutrients within agriculture. Such an approach may decrease the dependency of mineral-bound

Received: November 25, 2013
Revised: January 16, 2014
Published: January 21, 2014

Table 1. Elemental Composition of the Six Pelletized Fuels with Reference Values for Typical Sewage Sludge Composition; Main Ash-Forming Elements Are Shown, Together with Some Molar Ratios of Interest

	Elemental Composition (% (w/w) of d.s.)						
	Data from ref 28, average (min−max)	Biosolid A	Biosolid A + K (P:K = 1:1)	Biosolid A + K + Ca (P:K:Ca = 1:1:1)	Biosolid B	Biosolid B + K (P:K = 1:1)	Biosolid B + K + Ca (P:K:Ca = 1:1:1)
ash content[a] (% (w/w) of d.s.)	n.a.	35.0	38.0	40.1	38.9	43.1	44.6
LHV[b] (MJ/kg d.s.)	n.a.	13.8	13.6	12.7	13.3	12.7	12.0
elemental composition (%)							
K	0.44 (0.07−1.2)	0.42	3.90	4.03	0.32	5.40	4.34
Na	0.35 (0.08−3.0)	0.25	0.23	0.22	0.16	0.16	0.14
Ca	2.8 (0.62−19)	2.21	1.99	4.16	2.59	2.46	4.45
Mg	0.34 (0.08−0.63)	0.29	0.27	0.25	0.25	0.24	0.23
Al	4.0 (0.68−9.2)	5.50	5.13	4.78	1.71	1.60	1.48
Fe	4.9 (0.44−15)	2.83	2.52	2.35	10.07	9.44	8.81
Si	4.5 (1.6−15)	3.90	3.64	3.42	2.95	2.74	2.53
P	2.7 (1.1−5.5)	3.37	3.19	2.95	3.88	3.61	3.44
S	0.9 (0.42−2.6)	1.12	1.04	1.03	1.16	0.94	1.07
Cl	n.a.	0.046	0.044	0.042	0.026	0.020	0.019

	Molar Ratios[c]					
	Biosolid A	Biosolid A + K (P:K = 1:1)	Biosolid A + K + Ca (P:K:Ca = 1:1:1)	Biosolid B	Biosolid B + K (P:K = 1:1)	Biosolid B + K + Ca (P:K:Ca = 1:1:1)
P/K	10.06	1.03	0.92	15.15	0.85	1.00
P/(K + Ca)	1.65	0.69	0.46	1.72	0.59	0.50
P/Si	0.78	0.79	0.78	1.19	1.20	1.23
K/Al	0.05	0.53	0.58	0.13	2.32	2.02

[a]Ash content determined after ashing at 550 °C. [b]Lower heating value. [c]Calculated molar ratios in the pelletized fuels.

nutrient sources, which would benefit long-term sustainability in food production.

In order to create an efficient phosphorus recovery, it is important to concentrate as much of the phosphorus as possible to specific ash fractions, regardless of whether this ash is going to be used directly or further treated to a refined product. If an ash fraction such as fly ash from circulating fluidized beds or bed ash from bubbling fluidized beds is used directly as a fertilizer, having an ash fraction with high phosphorus imply that smaller amounts of ash need to be applied to reach the desired phosphorus amount per hectare. This also suggests adding less material with low nutritional value to the soil and that smaller amounts of elements that are potentially harmful to the environment would be distributed to the soil when less ash needs to be used to reach the same phosphorus fertilization. If the ash fraction is used in a workup process, having a high phosphorus content would suggest that less chemicals may be required to extract the same amount of phosphorus. It is also important to design the fuel blend in co-combustion, so that phosphorus can be found in a chemical form that is readily available for plants; this is vital for direct use of ash but also means that less chemicals may be needed in a phosphorus recovery/refinement process.

Fluidized-bed technology is a suitable method for sewage sludge combustion, where tolerance for fuel variations and complete fuel burnout are stressed as important features.[1,24] Experiments with co-combustion of biosolid in a circulating fluidized bed have been used to evaluate the distribution of main ash-forming elements and trace metals.[9,12,14,25,26] Phosphorus was enriched in the fly ashes, where it was found together with significant levels of several trace metals that are harmful to the environment.[27] Compared to circulating fluidized beds (CFBs), a bubbling fluidized bed may retain a larger part of the total ash in the bed ash fraction and separates volatile ash components into the flue gas better than a CFB, providing a higher degree of ash fractionation. Pelletizing or granulating fuels or mixtures containing biosolids may help fuel particles endure the abrasive environment to form ash pellets during combustion. The formation of such ash particles with a large part of the fuel ash and high phosphorus content was observed during co-combustion of wheat straw with biosolids in a bubbling fluidized bed.[14] It should be pointed out that it is important to consider the overall ash chemistry to enrich phosphorus in the bed ash particles and also reduce the amount of volatile and potentially harmful elements in the bed ash, such as mercury and cadmium.

To explore this approach to phosphorus recovery, it is important to investigate how the ash from pelletized biosolids is distributed in a bubbling fluidized-bed furnace, in which the ash fraction of phosphorus can be found, and in which the chemical form it is present. In addition, it is important to see if the alkali and alkaline-earth metal content in potential co-combustion fuel blends will affect phosphorus speciation.

The aim of this paper is to discuss (i) the distribution of phosphorus and other main ash-forming elements when combusting pelletized biosolids in a bubbling fluidized bed; (ii) in which chemical form these elements can be found; and (iii) how biosolid ash affects combustion properties. Environmentally harmful elements and leaching characteristics will be discussed and further evaluated in a second paper, and a third paper will discuss how biosolid ash compares to other fertilizers in plant growth experiments.

2. MATERIALS AND METHODS

2.1. Fuels and Additives. The biosolids used in this study were digested municipal sewage sludge from two different wastewater treatment facilities, and also two chemical additives were used to investigate how an increase of alkali and alkaline-earth metal content

dx.doi.org/10.1021/ef402320q | Energy Fuels 2014, 28, 1183−1190

affects the ash chemistry, which is related to co-combustion properties with biomass fuels. Potassium and calcium were used since it is well-known that these elements play important roles in biomass ash chemistry, where potassium is considered problematic and calcium may remedy ash-related problems. Different precipitation agents were used for the two types of biosolids during the wastewater treatment process. Biosolid A, retrieved at the municipal wastewater treatment facility in Tuvan, Skellefteå, Sweden, was precipitated with polyaluminum hydroxychloride (PAC) (Ekoflock 91, Eka Chemicals) and Biosolid B retrieved at the municipal wastewater treatment facility on Ön, Umeå, Sweden was precipitated with iron(II) sulfate ($FeSO_4$) (COP, Kemira). Biosolid A was obtained as pellets that had undergone hygienization with a water content of ∼20% and Biosolid B was acquired as dehydrated sludge with a water content of ∼60%. Biosolid B was further dried at ∼130 °C until the water content had reached ∼10%.

The two raw materials were milled and pelletized in three different fractions; one fraction containing the unmodified sewage sludge, one fraction with addition of K_2CO_3 (>98% Fisher Scientific), and one fraction with addition of both K_2CO_3 and $CaCO_3$ (>98%, Fisher Scientific). The additives were introduced to achieve a 1:1 molar ratio between P and K in the first blend and 1:1:1 molar ratio between P, K, and Ca in the latter case. These molar ratios were chosen to see whether potassium could be included in ternary phosphates. Rapeseed oil (∼3% (w/w)) and water were added to the raw materials to facilitate the pelletizing process. This resulted in six types of 6 mm (diameter) pellets with good durability during the fuel feed. The elemental composition for the six types are shown in Table 1 including reference values[28] for typical sewage sludge elemental composition in Sweden.

2.2. Low-Temperature Ashing. Since previous work suggests that aluminosilicates in the form of zeolites may be important for the capture of alkali metals,[29] it is of interest to clarify whether the two biosolids used in this study contain zeolites. Pellets of Biosolids A and B were subjected to low-temperature ashing at 120 °C in a Quorum Technologies, Ltd., Model PT7160 RF plasma barrel etcher, using an oxygen and argon atmosphere until no weight change could be observed. The resulting ash was then analyzed semiquantitatively with XRD to identify the compounds that were present.

2.3. Combustion Experiments. A 2-m-high benchscale bubbling fluidized bed with an inner bed diameter of 100 mm and a freeboard inner diameter of 200 mm was used for the combustion experiments. The bed material was quartz (>98%) with a grain size of 200−250 μm. Fuel feeding of 6 mm diameter pellets with a length of 5−25 mm was continuous. The combustion period lasted for 75 min or until bed defluidization occurred, since the high ash content of the pellets made longer combustion periods unsustainable in the experimental setup which did not have the possibility of ash removal. During this time, the oxygen level was kept at 8%−10% with a fluidization velocity ∼10 times the minimum fluidization velocity (∼1 m/s). The experiments were carried out at an effect of ∼2.5 kW at two different bed temperatures for each mixture: 800 and 950 °C. The freeboard section of the furnace was kept at the same temperature as the bed, using electrical heaters. The bed material and cyclone ash (>10 μm cutoff particle size in the cyclone) was collected after cooling. Particulate matter sampling was made using total dust Teflon filters, allowing for subsequent qualitative analysis of K, Na, P, S, and Fe.

2.4. Ash Fractions—Quantitative and Qualitative Analysis. The ash distributed between bed ash, cyclone ash, and total particulate matter (PM-tot) were weighed and subjected to elemental analysis (all ash fractions) and XRD analysis (large bed ash particles). The large bed ash particles represents a bed ash fraction that was sieved out of the bed ash with a considerably larger sieving particle size than the bed material (>1.2 mm, compared to the 0.200−0.250 mm of sieved bed material). Another bed ash particle fraction in the range of 0.300−1.2 mm was sieved in order to improve the closure of the mass balance. The large bed ash particles (>1.2 mm) were analyzed both qualitatively, using X-ray fluorescence (XRF) for Cl and inductively coupled plasma−atomic emission spectroscopy−section-field mass spectroscopy (ICP-AES/SFMS) for other elements, according to modified EPA methods 200.7 and 200.8 with three replicates, and quantitatively, using XRD. Elemental analysis was carried out with SEM-EDS for the smaller bed ash particle fraction ($0.300 < x < 1.2$ mm) and the remaining bed material containing both ash and bed sand was not subjected to further analysis in this study. Elemental analysis of the smaller bed ash fraction and the cyclone ash was made using SEM-EDS on a Philips XL30 electron microscope equipped with an EDAX energy dispersive detector. Samples were mounted on a carbon tape and three representative areas were analyzed, the size of these areas varied somewhat with analysis area side lengths in the range of 200−750 μm, depending on the sample amount and distribution on the carbon tape. Total particulate matter Teflon filter (PM-tot) analysis was performed via ICP-AES, according to modified EPA methods 200.7 and 200.8 for K, Na, P, S, and Fe. The sample preparation procedure for Teflon filters did not allow for a more extensive elemental analysis. The XRD analysis of ash from low-temperature ashing and for large bed ash particles was made with a Bruker-AXS d8 Avance X-ray diffractometer using Cu Kα radiation and a Våntec-1 detector. Compounds were identified using Diffrac^{plus} EVA[30] with the PDF-2[31] database. The diffractograms were further analyzed in Diffrac^{plus} TOPAS,[32] using Rietveld refinement techniques with reference data from ICSD[33] for a semiquantitative analysis of the crystalline matter in these samples.

3. RESULTS AND DISCUSSION

3.1. Raw Material. No evidence of zeolite presence was found in the XRD analysis of ashes from low-temperature treatment of either biosolid (see Table 2). This implies that there are, at most, trace amounts of zeolites originating from detergents or other sources. Silicates containing aluminum and alkali, such as microcline and albite, were identified. For the sludge precipitated with iron(II) sulfate, some hematite was also found. As can be seen in the diffractogram (see Figure 1), the prominent peaks, and, for zeolites, typical peaks[34−36] in the 2θ range of 15°−20° are absent. If zeolites are present in

Table 2. Results from the Semiquantitative XRD Analysis of Low-Temperature Ashed Material

	Content (%, w/w)	
	Biosolid A	Biosolid B
quartz	40	52
albite	39	16
microcline	21	27
hematite		5

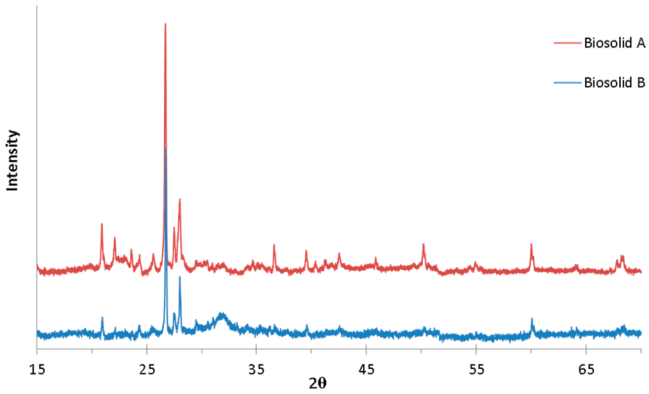

Figure 1. Diffractogram from XRD analysis of ash from low-temperature ashing. The area from 15°−20 2θ° lacks any clear peaks that should have been present with zeolites in the ash samples.

dx.doi.org/10.1021/ef402320q | Energy Fuels 2014, 28, 1183−1190

biosolids, they are likely to be associated with cations, such as sodium or calcium, so when biosolids are used in co-combustion, the importance of zeolites as an alkali adsorbent is probably smaller than has been suggested in previous publications.[11,37] There are trace amounts of other compounds, which could not be positively identified, which is most evident with the broad peak in Biosolid B in the 2θ range of 30°−32° with overlaid peaks belonging to other compounds.

3.2. Ash Distribution. The ash distribution in the bubbling fluidized bed is shown in Figure 2. When sieving the bed ash particle fraction (>1.2 mm) it was noticed that the bulk of the bed ash particles appeared to have survived the abrasive conditions in the bubbling bed, since the cylindrical pellet shape was retained for the ash particles after burn out (see Figure 2). The rest fraction in the total mass balance (Figure 2) is dominated by bed ash that has a sieving particle size smaller than 0.300 mm. Sieving more bed ash by working with smaller sizes would cause a large error in total mass, because of the increased inclusion of bed material.

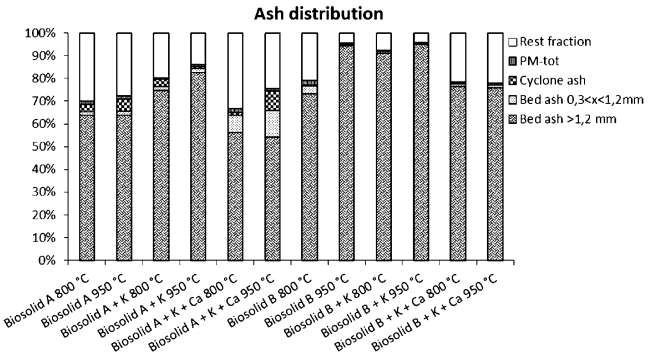

Figure 2. Mass distribution of ash between different ash fractions.

Large bed ash particles, such as those shown in Figure 3, comprised 54%−95% (w/w) of the total ash content. This shows a high degree of retention of nonvolatile main ash forming elements in the bed ash, preferentially in the large bed ash particles. These "ash pellets" were more brittle for Biosolid A than the ones formed by Biosolid B. That affected the amount of cyclone ash and particulate matter—Biosolid A produced a much larger cyclone ash fraction than Biosolid B in general. The amounts of particulate matter show similar trends. The rest fraction, which mainly consisted of bed ash particles smaller than 0.300 mm and some material sticking to the reactor walls, was also larger for biosolid A. Since one of the largest differences between biosolids A and B is their respective precipitation chemicals, PAC and iron(II) sulfate, the variations in durability of the ash pellets, as judged by relative mass in the large bed ash fraction, could originate from the large difference in aluminum and iron content. Even if that is the case, it cannot be stated with certainty, based on this study, if sludge precipitated with one chemical is to prefer over sludge precipitated with another. The larger mass fraction kept in "ash pellets" for biosolid B could possibly indicate some melt formation within the ash particles whereas ash from biosolid A could have a higher overall melting point despite being more brittle which of course is important from a bed agglomeration point of view particularly when considering co-combustion. An in-depth study of this effect of aluminum and iron is beyond the scope of the work presented here.

Figure 3. Example of "ash pellets". These were formed during the combustion of Biosolid B with the addition of K_2CO_3 at 800 °C.

3.3. Main Ash-Forming Elements. The main ash-forming elements are here considered to be K, Na, Ca, Mg, Al, Fe, Si, P, S, and Cl. First, the distribution and speciation of phosphorus will be discussed in detail, followed by the other anion (Lewis base) formers (Si, S, Cl). Elements forming positive ions will be mentioned based on what ionic charge they have. Brief comments on melting points are included for elements which are considered to benefit problematic fuels in co-combustion since melting points are important for bed agglomeration and slag formation.

Phosphorus was found to be enriched in the large bed ash particles proportionally to the amount introduced with the fuel (see Figure 4). The main phosphorus-containing compound identified in the bed was a whitlockite (see Table 3). This specific structure is fairly accommodating regarding which cations can be incorporated. Both $Ca_9Fe(PO_4)_7$ and $Ca_9KMg(PO_4)_7$ have been identified previously.[9] These limited solid solutions result in almost identical diffractograms which hampers the possibility to distinguish between different compositions due to small changes in their crystal structure. No certain composition of the whitlockite found in this study can be assigned, based on present observations, but altogether we find the whitlockite compounds suggested above to be likely candidates. From the literature[38−43] it is evident that whitlockite can act as host structure for a larger number of divalent, monovalent, and trivalent cations. Apparently, properties of the whitlockite crystal structure admit complicated but restricted solid solutions. Whitlockite will most likely serve as an important host phase for alkali metal retention which is one of the interesting aspects of using biosolid for co-combustion. However, there is a risk that some environmentally harmful elements also may be retained due to flexibility of the positive cat-ion sites in this structure

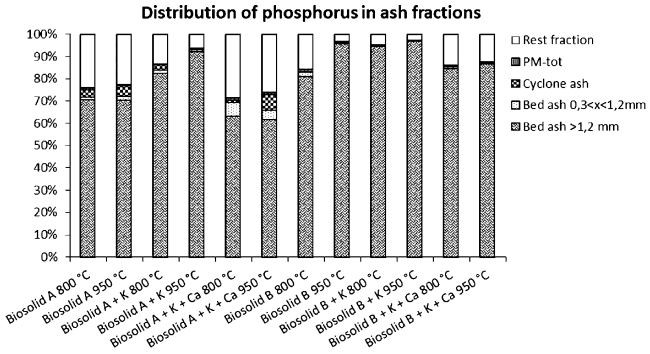

Figure 4. Distribution of phosphorus from the fuel between the different ash fractions.

As previously mentioned, silicon is present as both quartz and two feldspar minerals in biosolid raw materials. When the

dx.doi.org/10.1021/ef402320q | Energy Fuels 2014, 28, 1183−1190

Table 3. Semiquantitative Analysis of Crystalline Phases in Bed Ash Particles Larger than 1.2 mm

	Biosolid A		Biosolid A + K, P:K = 1:1		Biosolid A + K + Ca, P:K:Ca = 1:1:1		Biosolid B		Biosolid B + K, P:K = 1:1		Biosolid B + K + Ca, P:K:Ca = 1:1:1	
	800 °C	950 °C	800 °C	950 °C	800 °C	950 °C	800 °C	950 °C	800 °C	950 °C	800 °C	950 °C
whitlockite	31	45	35	27	46	53	29	20	26	12	26	32
quartz	22	12	18	16	14	8	21	16	9	13	10	7
cristobalite	10	13					11	11				
plagioclase	7	16	6		11	2	8	14	9	9	11	5
microcline	19	2	17		16	9	20	6	2	7	13	3
leucite				43		11			11	23		17
arkanite			17	4	4	7			14	9	8	6
anhydrite					3							
hematite	1	8	7	10	6	10	2	33	29	27	32	30
maghemite	10	4					9					

unmodified fuels (no additive) are combusted there is some formation of cristobalite, which indicate that there are Lewis bases other than silica that will react with the cations present in the fuel. Cristobalite has previously been identified for instance when using additives with wheat straw and fuels containing husks.[18,44] As the amount of cations is increased by the use of additives, cristobalite cannot be identified in the large bed ash particles. Instead a shift is seen toward the formation of albite, microcline, and leucite. The leucite is mainly produced in the 950 °C experiments, and with addition of only K_2CO_3 to each biosolid.

Sulfur and chlorine are more volatile Lewis base precursors, forming sulfates and chlorides, respectively. The large rest fraction shown in Figure 5 can be found either in bed ash or in

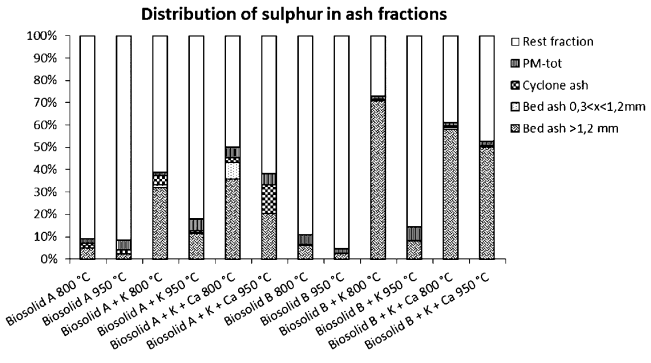

Figure 5. Distribution of sulfur from the fuel between the different ash fractions.

flue gas, primarily as sulfur dioxide gas (SO_2 (g)). For all mixtures where K_2CO_3 was added, K_2SO_4 formed in large bed ash particles. Trace amounts of $CaSO_4$ could be found after combustion at 800 °C for biosolid A after addition of both K_2CO_3 and $CaCO_3$. When this mixture was combusted at 950 °C, this trace amount had disappeared and the crystalline amount of K_2SO_4 increased slightly in the bed while the sulfur amount in PM-tot also increased. This shows the high potential for alkali capture by sulfur present in biosolids. An increase in combustion temperature generally decreased the amount of sulfur that was found in the bed. There was no trace of chlorine in the large bed ash particles but small amounts could be found in the cyclone ash. It is likely that most of the chlorine has been volatilized as HCl.

Potassium and sodium as alkali metals display a slight difference in behavior. Both are mostly retained in the large bed ash particles by reaction with various Lewis bases (see Table 3, as well as Figures 6 and 7). The calculated sodium content

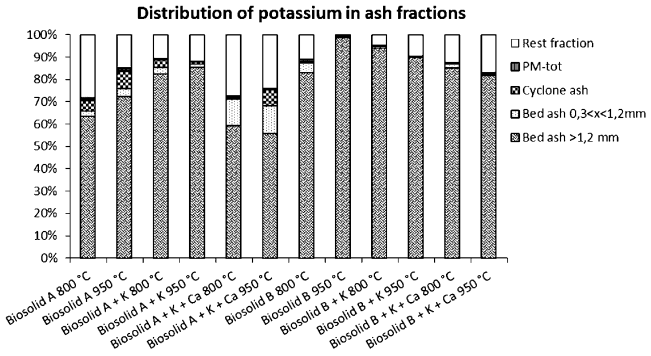

Figure 6. Distribution of potassium from the fuel between the different ash fractions.

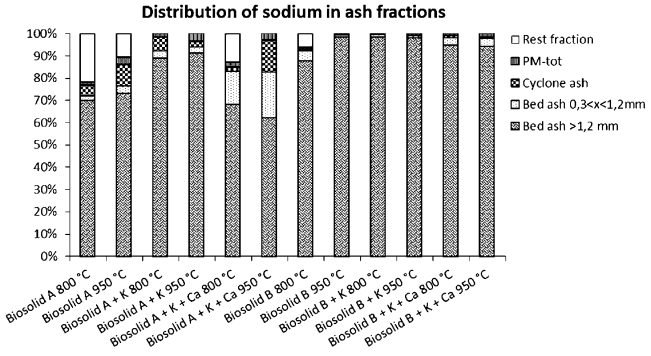

Figure 7. Distribution of sodium from the fuel between the different ash fractions.

based on fuel analyses underestimated the total sodium content, compared to ash fraction samples, shown in Figure 6 as a lack of rest fraction. The sodium concentration in total particulate matter increases at the higher combustion temperature to always surpass the potassium concentration, even in the experiments where K_2CO_3 has been added to the biosolids. This suggests a more efficient retention of potassium in the bed

dx.doi.org/10.1021/ef402320q | Energy Fuels 2014, 28, 1183−1190

ash and, to some extent, in the cyclone ash at higher bed temperatures.

Calcium and magnesium were largely found in bed ash particles and, to some extent, in cyclone ash (see Figures 8 and

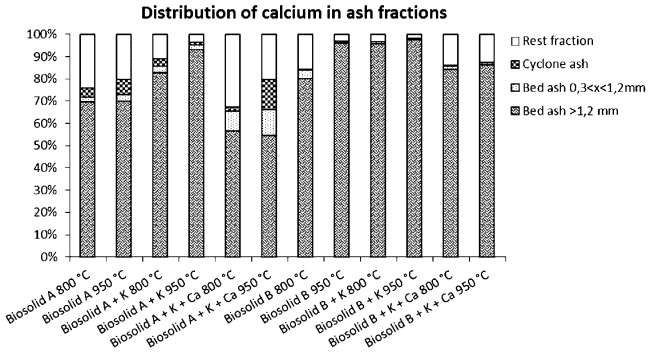

Figure 8. Distribution of calcium from the fuel between the different ash fractions.

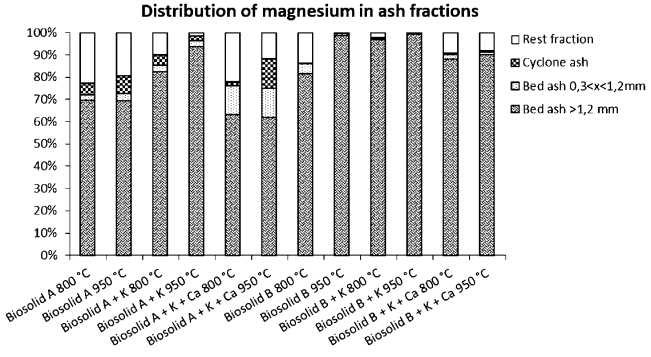

Figure 9. Distribution of magnesium from the fuel between the different ash fractions.

9). This distribution is consistent with that contributed by these alkaline-earth elements toward increasing the melting point when included in feldspars such as albite and reducing volatility and melting points of phosphorus compounds. The transport of calcium and magnesium from the bed should mainly be attributed to entrainment of small bed ash particles with flue gas rather than condensation from a gas phase, which could be the case for alkali metals. The brittle ash particles produced by Biosolid A emphasizes this mass transport from bed to cyclone ash while very little Ca and Mg is found in cyclone ash or later in the system for Biosolid B. This abundance of calcium in particular that may increase the overall melting temperature of bed ash is of great importance when considering co-combustion of biosolids with more problematic fuels.

Aluminum is mainly found in bed ash and the rest fraction, plausibly increasing the melting point of the silicate systems found in this study (see Table 3 and Figure 10). In the cases where additives were used with biosolids, the phase leucite ($KAlSi_2O_6$) was formed at 950 °C for both biosolids and at 800 °C for Biosolid B with the addition of K_2CO_3. The silica phase cristobalite disappears with the addition of potassium to the biosolids for all mixtures and temperatures. In order to form leucite, aluminum in some form (e.g., chloride from precipitation agent) must react with silica and potassium compounds. An alternative formation path may be a reaction

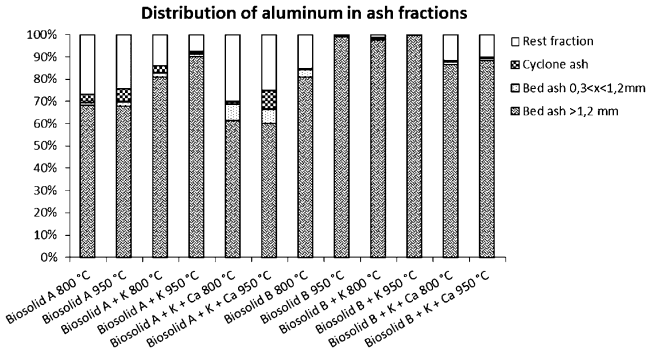

Figure 10. Distribution of aluminum from the fuel between the different ash fractions.

where feldspars, microcline in this study, reacts with aluminum and potassium compounds. Since leucite is formed under these conditions, it may be concluded that it is more stable than ternary Ca−K-phosphates. The complete speciation of inherent aluminum in biosolids cannot be deduced based on results in the present study.

Iron in the biosolid material typically oxidizes to Fe^{3+}, which is evident from observed amounts of Fe_2O_3, a change that is promoted by higher temperature. At 950 °C, all iron identified by XRD is found as hematite. Another iron(III) species that occurs in small amounts at 800 °C for some mixtures is maghemite which also has the sum formula (Fe_2O_3). There may exist iron in the whitlockite $Ca_9Fe(PO_4)_7$; however, as discussed above, this cannot be stated with certainty.

Based on these bench-scale experiments it is likely that biosolids could be combusted in a full-scale bubbling fluidized bed to produce a bed ash fraction which contains most of the phosphorus introduced with the fuel where a pretreatment step to produce durable bed ash particles after fuel burn-out possibly could increase phosphorus recovery. Some alkali may be retained in the bed ash in aluminum silicates where the aluminum content contributes to higher melting points of alkali-containing aluminum silicates in the bed ash. Calcium and magnesium have the same positive effects when included in the silicate structure. This suggests that some waste streams from agriculture where bed agglomeration can be attributed to alkali silicate melt formation could be an alternative when considering co-combustion with biosolids in bubbling fluidized beds. The high amount of sulfur in biosolids could possibly prevent of alkali chloride formation in the flue gas by sulfate formation instead. Since the amount of biosolids or undigested municipal sewage sludge available could be a limiting factor for full-scale systems it is important to investigate which co-combustion biomasses that may be suitable and the effect of changing the ratio of biosolids to biomass in such co-combustion mixtures. Studies on the pretreatment process are needed to increase the amount of material staying in a large bed ash fraction which would also facilitate phosphorus recovery.

4. CONCLUSIONS

Results in this study suggest that combustion of prepelletized/granulated biosolids in bubbling fluidized beds, possibly co-fired with other K- and Ca-rich biomass fuels, could be a suitable technique for recovering macronutrients such as phosphorus from this waste stream.

- Large bed ash particles were found to contain a large part of the ash where the biosolid forming the hardest bed ash

dx.doi.org/10.1021/ef402320q | Energy Fuels 2014, 28, 1183−1190

also gave the highest yield of ash pellets. Fuel pretreatment such as pelletizing or granulation may therefore be important for higher phosphorus recovery yields from specific ash fractions.

- Concentrations of main ash-forming elements other than chlorine are increased in bed ash compared to those found in total ash content, meaning that combustion acts as an enrichment process. Phosphorus in particular was enriched in bed ash pellets in proportion to the amount introduced with the fuel.
- Phosphorus was found as a whitlockite and a solid solution with a composition similar to $Ca_9(Fe,K,Mg)(PO_4)_7$ is a likely candidate. Potassium addition resulted in the formation of leucite ($KAlSi_2O_6$) at high temperatures and some arcanite (K_2SO_4) formation for all fuel blends. The only observed effect of calcium addition was generally increased levels of whitlockite for Biosolid A and at 950 °C for Biosolid B. The silica phase cristobalite present in ash from unmodified biosolids was not identified in the fuel blends, suggesting aluminum silicate formation as a result of the alkali and alkaline-earth metal addition.
- The absence of zeolites in ash from low-temperature ashing suggests that the role of zeolites as alkali adsorbent during combustion of biosolids is insignificant, whereas the overall aluminum content in conjunction with reactive silica is important.

AUTHOR INFORMATION

Corresponding Author

*E-mail: nils.skoglund@umu.se.

Notes

The authors declare no competing financial interest.

ACKNOWLEDGMENTS

The authors would like to gratefully acknowledge the financial support of the Swedish Research Council (VR), Swedish Water & Wastewater Association, the North Waste Infrastructure Project, Swedish Energy Agency (STEM), and National (Swedish) Strategic Research Program Bio4Energy.

REFERENCES

(1) Werther, J.; Ogada, T. Sewage sludge combustion. *Prog. Energy Combust. Sci.* **1999**, *25*, 55−116.

(2) Rulkens, W. Sewage Sludge as a Biomass Resource for the Production of Energy: Overview and Assessment of the Various Options. *Energy Fuels* **2007**, *22*, 9−15.

(3) Fytili, D.; Zabaniotou, A. Utilization of sewage sludge in EU application of old and new methods—A review. *Renewable Sustainable Energy Rev.* **2008**, *12*, 116−140.

(4) Tyagi, V. K.; Lo, S.-L. Sludge: A waste or renewable source for energy and resources recovery? *Renewable Sustainable Energy Rev.* **2013**, *25*, 708−728.

(5) Zhang, F.-S.; Yamasaki, S.; Nanzyo, M. Waste ashes for use in agricultural production: I. Liming effect, contents of plant nutrients and chemical characteristics of some metals. *Sci. Total Environ.* **2002**, *284*, 215−225.

(6) Lindberg, R. H.; Fick, J.; Tysklind, M. Screening of antimycotics in Swedish sewage treatment plants−Waters and sludge. *Water Res.* **2010**, *44*, 649−657.

(7) Olofsson, U.; Bignert, A.; Haglund, P. Time-trends of metals and organic contaminants in sewage sludge. *Water Res.* **2012**, *46*, 4841−4851.

(8) Clarke, B. O.; Smith, S. R. Review of "emerging" organic contaminants in biosolids and assessment of international research priorities for the agricultural use of biosolids. *Environ. Int.* **2011**, *37*, 226−247.

(9) Pettersson, A.; Åmand, L. E.; Steenari, B. M. Leaching of ashes from co-combustion of sewage sludge and wood—Part I: Recovery of phosphorus. *Biomass Bioenergy* **2008**, *32*, 224−235.

(10) Eichler-Loebermann, B.; Schiemenz, K.; Makadi, M.; Vago, I.; Koeppen, D. Nutrient Cycling by Using Residues of Bio-Energy Production—Effects of Biomass Ashes on Plant and Soil Parameters. *Cereal Res. Commun.* **2008**, *36*, 1259−1262.

(11) Åmand, L. E.; Leckner, B.; Eskilsson, D.; Tullin, C. Deposits on heat transfer tubes during co-combustion of biofuels and sewage sludge. *Fuel* **2006**, *85*, 1313−1322.

(12) Elled, A. L.; Åmand, L. E.; Leckner, B.; Andersson, B. A. Influence of phosphorus on sulphur capture during co-firing of sewage sludge with wood or bark in a fluidised bed. *Fuel* **2006**, *85*, 1671−1678.

(13) Elled, A. L.; Davidsson, K. O.; Åmand, L. E. Sewage sludge as a deposit inhibitor when co-fired with high potassium fuels. *Biomass Bioenergy* **2010**, *34*, 1546−1554.

(14) Skoglund, N.; Grimm, A.; Öhman, M.; Boström, D., Effects on Ash Chemistry when Co-firing Municipal Sewage Sludge and Wheat Straw in a Fluidized Bed: Influence on the Ash Chemistry by Fuel Mixing. *Energy Fuels* **2013**.

(15) Li, L.; Ren, Q.; Li, S.; Lu, Q. Effect of Phosphorus on the Behavior of Potassium during the Co-combustion of Wheat Straw with Municipal Sewage Sludge. *Energy Fuels* **2013**, *27*, 5923−5930.

(16) Vainio, E.; Yrjas, P.; Zevenhoven, M.; Brink, A.; Laurén, T.; Hupa, M.; Kajolinna, T.; Vesala, H. The fate of chlorine, sulfur, and potassium during co-combustion of bark, sludge, and solid recovered fuel in an industrial scale BFB boiler. *Fuel Process. Technol.* **2013**, *105*, 59−68.

(17) Boström, D.; Skoglund, N.; Grimm, A.; Boman, C.; Öhman, M.; Broström, M.; Backman, R. Ash Transformation Chemistry during Combustion of Biomass. *Energy Fuels* **2012**, *26*, 85−93.

(18) Grimm, A.; Skoglund, N.; Boström, D.; Öhman, M. Bed Agglomeration Characteristics in Fluidized Quartz Bed Combustion of Phosphorus-Rich Biomass Fuels. *Energy Fuels* **2011**, *25*, 937−947.

(19) Grimm, A.; Skoglund, N.; Boström, D.; Boman, C.; Öhman, M. Influence of Phosphorus on Alkali Distribution during Combustion of Logging Residues and Wheat Straw in a Bench-Scale Fluidized Bed. *Energy Fuels* **2012**, *26*, 3012−3023.

(20) Lindström, E.; Sandström, M.; Boström, D.; Öhman, M. Slagging characteristics during combustion of cereal grains rich in phosphorus. *Energy Fuels* **2007**, *21*, 710−717.

(21) Piotrowska, P.; Zevenhoven, M.; Davidsson, K.; Hupa, M.; Åmand, L. E.; Barisic, V.; Zabetta, E. C. Fate of Alkali Metals and Phosphorus of Rapeseed Cake in Circulating Fluidized Bed Boiler. Part 1: Cocombustion with Wood. *Energy Fuels* **2010**, *24*, 333−345.

(22) Piotrowska, P.; Grimm, A.; Skoglund, N.; Boman, C.; Öhman, M.; Zevenhoven, M.; Boström, D.; Hupa, M. Fluidized-Bed Combustion of Mixtures of Rapeseed Cake and Bark: The Resulting Bed Agglomeration Characteristics. *Energy Fuels* **2012**, *26*, 2028−2037.

(23) Vassilev, S. V.; Baxter, D.; Andersen, L. K.; Vassileva, C. G.; Morgan, T. J. An overview of the organic and inorganic phase composition of biomass. *Fuel* **2012**, *94*, 1−33.

(24) Van Caneghem, J.; Brems, A.; Lievens, P.; Block, C.; Billen, P.; Vermeulen, I.; Dewil, R.; Baeyens, J.; Vandecasteele, C. Fluidized bed waste incinerators: Design, operational and environmental issues. *Prog. Energy Combust. Sci.* **2012**, *38*, 551−582.

(25) Åmand, L. E.; Leckner, B.; Eskilsson, D.; Tullin, C. Deposits on heat transfer tubes during co-combustion of biofuels and sewage sludge. *Fuel* **2006**, *85*, 1313−1322.

(26) Davidsson, K. O.; Åmand, L. E.; Elled, A. L.; Leckner, B. Effect of cofiring coal and biofuel with sewage sludge on alkali problems in a circulating fluidized bed boiler. *Energy Fuels* **2007**, *21*, 3180−3188.

(27) Pettersson, A.; Åmand, L. E.; Steenari, B. M. Leaching of ashes from co-combustion of sewage sludge and wood. Part II: The mobility

of metals during phosphorus extraction. *Biomass Bioenergy* **2008**, *32*, 236−244.
(28) Eriksson, J. *Concentrations of 61 trace elements in sewage sludge, farmyard manure, mineral fertiliser, precipitation and in oil and crops*; Swedish Environmental Protection Agency Report 5159; Swedish Environmental Protection Agency, 2001.
(29) Pettersson, A.; Åmand, L.-E.; Steenari, B.-M. Chemical fractionation for the characterisation of fly ashes from co-combustion of biofuels using different methods for alkali reduction. *Fuel* **2009**, *88*, 1758−1772.
(30) *Diffrac^{plus} EVA 10.0*; Bruker AXS Gmbh: Karlsruhe, Germany, 2003.
(31) *Powder Diffraction File*, PDF-2. International Center for Diffraction Data (ICDD): Newtowne Square, PA, 2004.
(32) *Diffrac^{plus} TOPAS 2.1*; Bruker AXS Gmbh: Karlsruhe, Germany, 2003.
(33) Inorganic Crystal Structure Database online (ICSD Web). National Institute of Standards and Technology, Fachinformationzentrum Karlsruhe: Karlsruhe, Germany.
(34) Yanagida, R. Y.; Amaro, A. A.; Seff, K. Redetermination of the crystal structure of dehydrated zeolite 4A. *J. Phys. Chem.* **1973**, *77*, 805−809.
(35) Armstrong, A. R.; Anderson, P. A.; Woodall, L. J.; Edwards, P. P. Structure of NA-4(3+) in Sodium Zeolite Y. *J. Am. Chem. Soc.* **1995**, *117*, 9087−9088.
(36) Turner, S.; Sieber, J. R.; Vetter, T. W.; Zeisler, R.; Marlow, A. F.; Moreno-Ramirez, M. G.; Davis, M. E.; Kennedy, G. J.; Borghard, W. G.; Yang, S.; Navrotsky, A.; Toby, B. H.; Kelly, J. F.; Fletcher, R. A.; Windsor, E. S.; Verkouteren, J. R.; Leigh, S. D. Characterization of chemical properties, unit cell parameters and particle size distribution of three zeolite reference materials: RM 8850 − zeolite Y, RM 8851 − zeolite A and RM 8852 − ammonium ZSM-5 zeolite. *Microporous Mesoporous Mater.* **2008**, *107*, 252−267.
(37) Pettersson, A.; Zevenhoven, M.; Steenari, B. M.; Åmand, L. E. Application of chemical fractionation methods for characterisation of biofuels, waste derived fuels and CFB co-combustion fly ashes. *Fuel* **2008**, *87*, 3183−3193.
(38) Morozov, V. A.; Presniakov, I. A.; Belik, A. A.; Khasanov, S. S.; Lazoryak, B. I. Crystal structures of calcium magnesium alkali metal phosphates $Ca_9MgM(PO_4)_7$ (M = Li, Na, K). *Crystallogr. Rep.* **1997**, *42*, 758−769.
(39) Gopal, R.; Calvo, C. Structural relationship of whitlockite and beta-$Ca_3(PO_4)_2$. *Nat. Phys. Sci.* **1972**, 237.
(40) Kannan, S.; Goetz-Neunhoeffer, F.; Neubauer, J.; Pina, S.; Torres, P. M. C.; Ferreira, J. M. F. Synthesis and structural characterization of strontium- and magnesium-co-substituted beta-tricalcium phosphate. *Acta Biomater.* **2010**, *6*, 571−576.
(41) Schroeder, L. W.; Dickens, B.; Brown, W. E. Crystallographic studies of role of Mg as a stabilizing impurity in beta-$Ca_3(PO_4)_2$. 2. Refinement of Mg-containing beta-$Ca_3(PO_4)_2$. *J. Solid State Chem.* **1977**, *22*, 253−262.
(42) Lazoryak, B. I.; Morozov, V. A.; Belik, A. A.; Khasanov, S. S.; Shekhtman, V. S. Crystal structures and characterization of $Ca_9Fe(PO_4)_7$ and $Ca_9FeH_{0.9}(PO_4)_7$. *J. Solid State Chem.* **1996**, *122*, 15−21.
(43) Sandström, M. H.; Boström, D. $Ca_{10}K(PO_4)_7$ from single-crystal data. *Acta Crystallogr., Sect. E: Struct. Rep. Online* **2006**, *62*, I253−I255.
(44) Thy, P.; Jenkins, B. M.; Grundvig, S.; Shiraki, R.; Lesher, C. E. High temperature elemental losses and mineralogical changes in common biomass ashes. *Fuel* **2006**, *85*, 783−795.